INSTITUTE OF PHYSICS PUBLISHING JOURNAL OF PHYSICS B: ATOMIC, MOLECULAR AND OPTICAL PHYSICS

J. Phys. B: At. Mol. Opt. Phys. **36** (2003) 3835–3846 PII: S0953-4075(03)63450-4

Electron capture by protons and electron loss from hydrogen atoms in collisions with hydrocarbon and hydrogen molecules in the 60–120 keV energy range

J M Sanders, S L Varghese, C H Fleming[1] and G A Soosai[2]

Department of Physics, University of South Alabama, Mobile, AL 36688, USA

E-mail: jsanders@jaguar1.usouthal.edu

Received 13 May 2003
Published 29 August 2003
Online at stacks.iop.org/JPhysB/36/3835

Abstract

Cross sections for electron capture by 60–120 keV protons and electron loss from 60–120 keV hydrogen atoms in collisions with molecular hydrogen, methane (CH_4), acetylene (C_2H_2), ethylene (C_2H_4), ethane (C_2H_6), propylene (C_3H_6), and propane (C_3H_8) have been measured. We found that the capture and loss cross sections depend linearly on the number of carbon atoms and the number of hydrogen atoms in the target molecules, as predicted by the simple additivity rule. The success of the additivity rule allowed the extraction of effective electron capture and loss cross sections for atomic hydrogen and atomic carbon targets.

1. Introduction

Collisions involving carbon-containing molecular targets as well as atomic carbon targets are of interest in several fields. To name just one area of application, in medical physics, collisions of protons and hydrogen atoms with carbon-bearing biological molecules are of particular application in proton therapy. In this therapy, the protons initially have high energies (several megaelectronvolts), but they come to rest in the body, so an understanding of proton–molecule collisions at much lower energies (several kiloelectronvolts) is very relevant to the technique. However, in all applications, the molecules are difficult to treat theoretically, since they are inherently many-body targets. For this reason, cross sections for collisions involving molecular targets are often related to cross sections for atomic targets by assuming that the molecular cross section is the sum of the cross sections of its constituent atoms. This assumption is called the additivity rule. Originally devised for stopping powers, the rule has been applied to cross sections for a wide variety of processes from x-ray absorption to electron capture.

[1] Present address: Department of Physics, University of Maryland, College Park, MD 20742, USA.
[2] Present address: School of Applied Physics, National University of Malaysia, Bangai, Selangor, Malaysia.

In this paper, we will focus on the application of the additivity rule to electron capture by protons and electron loss from hydrogen atoms colliding with hydrocarbon molecules at intermediate energies ($\sim$100 keV u^{-1}).

For electron capture, the additivity rule is expected to be limited to relatively high energies. A slow collision is dominated by the formation of molecular orbitals between the collision partners, the details of the structure of different molecular targets must be taken into account, and the simple additivity rule is not expected to hold [1]. At higher energies, several investigations have been made over the years to test the validity of the additivity rule in the electron capture process [2–7]. These previous experiments concentrated on relatively high-energy ($\sim$1 MeV u^{-1} and higher) collisions of bare projectiles. Bissinger *et al* [4, 5] studied proton projectiles colliding with a variety of hydrocarbon gases at energies from 800 to 3000 keV. In these experiments, significant deviations from the additivity rule were observed, namely, the cross sections did not increase with the number of carbon atoms as strongly as the rule would predict. To explain the reduction in the capture cross section, it was proposed that the projectile might lose its captured electron in collisions with other atoms on its way out of the molecule. This proposed mechanism was called the 'exit effect'.

Dillingham *et al* [7] extended the investigation to F^{9+} and F^{8+} ions colliding with hydrocarbon gases for energies from 500 to 1500 keV u^{-1}. In this case, the additivity rule was found to be valid. However, unlike the case with H^+ projectiles, the loss cross sections for F^{9+} and F^{8+} projectiles are much smaller than the capture cross sections, so the exit effect would not be expected to affect the capture cross sections for these collisions. Rottmann *et al* [8] measured capture cross sections for 100–1500 keV C^+ projectiles on several atomic and molecular gases (including some hydrocarbons). They observed that the cross sections scaled linearly as a function of the bond length for diatomic targets or with the number of constituent atoms for polyatomic targets. This latter scaling is similar to the additivity rule, but it does not distinguish between the contributions that different atoms may make to the overall cross section.

The exit effect as described above depends strongly on the relative size of the loss and capture cross sections. For fast ($E > 300$ keV) protons, loss cross sections are typically at least two orders of magnitude greater than capture cross sections [2]. Since an electron captured by a high energy proton is very likely to be lost on the way out of the molecule, the exit effect will cause significant deviations from the additivity rule. In contrast to the case for fast protons, loss cross sections are generally an order of magnitude *smaller* than capture cross sections for fast ($E > 500$ keV u^{-1}) bare and hydrogen-like fluorine ions, and the exit effect is not significant [7]. For intermediate energy protons ($E \sim 100$ keV), loss cross sections are only a little larger than capture, and the exit effect should therefore be reduced compared to high energy protons. Such a reduction of the exit effect increases the likelihood that the additivity rule will be valid in the energy range (60–120 keV) of the measurements reported in this paper. One goal of this work was to test the prediction that the additivity rule will hold in this energy range.

In addition to investigating the additivity rule for electron capture by protons, we also made measurements testing the rule for electron loss from atomic hydrogen projectiles. Recently Watson *et al* [9] have shown that additivity holds for electron loss cross sections for 6 MeV u^{-1} Xe^{18+} colliding with a variety of molecules. In this collision system, electron capture cross sections are estimated to be about two orders of magnitude smaller than the loss cross sections. Thus it is unlikely that the Xe projectile, having lost an electron, would capture another on its way out of the molecule—that is, the exit effect is small. In the case of hydrogen projectiles discussed in this paper, loss cross sections are also larger than electron capture (though the difference is not as extreme as in the Xe case), so we expect exit effects to be small and the additivity rule to hold well.

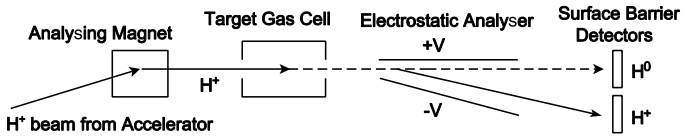

Figure 1. Schematic diagram of the experimental apparatus.

If the additivity rule is found to be valid for a particular collision system, it can be employed to obtain cross sections for the individual constituent atoms of the molecule. In its simplest form, the additivity rule states that the cross section for a collision between a projectile and a molecular target is simply the sum of the cross sections for collisions between the projectile and the constituent atoms of the molecule [4]. For example, the cross section for loss in a collision with a C_nH_m molecule would be

$$\sigma_l^{C_nH_m} = n\sigma_l^C + m\sigma_l^H \tag{1}$$

where σ_l^C and σ_l^H are the cross sections for loss in a collision with a carbon and hydrogen atom, respectively. A similar expression would apply to capture cross sections as well. After having established that the additivity rule holds in a particular energy range, we can use equation (1) to extract the cross sections for atomic targets. Obtaining atomic cross sections from data taken with molecular targets is a convenient strategy for materials such as carbon which are difficult to prepare as free atomic targets.

2. Experiment

A schematic diagram of the experimental apparatus is provided in figure 1. Proton beams with energies ranging from 60 to 120 keV were produced by a 150 kV Cockcroft–Walton accelerator. After passing through slits which collimate and control the projectile ion flux, the beam was momentum analysed by a 15° analysing magnet. The protons then passed through a differentially pumped target gas cell. The differential-pumping region was 19 cm long with entrance and exit apertures 4 mm in diameter and was pumped by a 600 l s^{-1} diffusion pump. The gas cell was mounted in the centre of the differential-pumping region; it was 2.76 cm long with entrance and exit apertures 1.8 mm in diameter. The flow of target gas into the cell was controlled by a leak valve, and the pressure in the cell was measured by a capacitance manometer.

Upon leaving the target gas cell, the projectile beam passed between the plates of an electrostatic analyser, which separated the H^+ and H^0 projectiles. The H^+ and H^0 projectiles were detected with surface barrier detectors, and the projectile count rate was limited to a maximum of 1000 s^{-1}, to minimize degradation of the detector efficiency and resolution. After being amplified, signals from the two detectors were pulse-height analysed (to facilitate setting noise discrimination levels and to monitor the beam energy), and stored by multichannel analysers. By comparing the count rates for the two detectors in both the H^+ and H^0 positions and with the electrostatic analyser on and off, it was found that each detector had the same efficiency for detecting H^+ and H^0. It was also ascertained that the efficiencies of the two detectors were equal to each other to within 3%.

Charge-state fractions of the H^+ and H^0 projectiles were measured as a function of gas cell pressure over a wide range of pressures, from very low, single-collision conditions, to very high, equilibrium conditions. The resulting charge fractions were then analysed using a two-charge-state model to obtain cross sections. The two charge states in this model were H^+ and H^0. Contributions from H^- were not included, since the fraction of the beam in the H^-

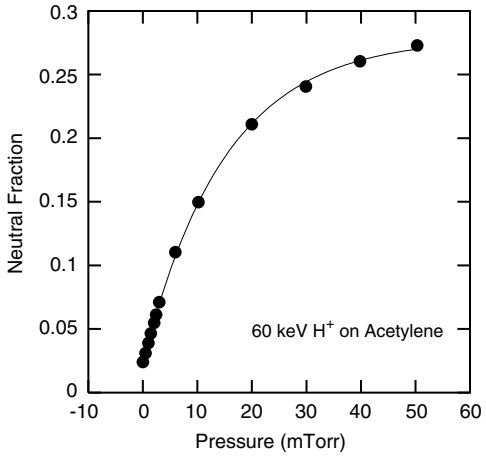

Figure 2. Neutral charge fraction versus pressure curve for 60 keV H^+ on acetylene. The full curve is the result of a non-linear least-squares fit of equation (2) to the data.

charge state at these energies is expected to be sufficiently small that contributions from H^- to the H^+ and H^0 charge state fractions may be neglected [2, 10, 11]. This expectation was verified for the case of a 60 keV H^+ beam on a C_3H_6 target by reversing the polarity of the electrostatic analyser, to allow the H^- beam to be directly measured. At its greatest, the H^- beam was less than 1.6% of H^0, and the charge fractions of H^0 computed with and without the H^- contribution differed by less than 1%.

The two-charge-state model yielded an expression for the H^0 beam fraction which was fitted to the data [12]:

$$f^0 = \frac{1}{1+R} + \left(f_0^0 - \frac{1}{1+R} \right) \exp[-s_c(1+R)P] \tag{2}$$

where f^0 is the charge-state fraction for the neutral species, f_0^0 is the background neutral fraction, R is the ratio of the cross section for loss to the cross section for capture, s_c is proportional to the cross section for capture by H^+, and P is the pressure of the target gas. When performing the non-linear least-squares fit, f_0^0, s_c, and R were the fitting parameters. An example of a fit of equation (2) to experimental neutral fractions is shown in figure 2. The cross section for capture by protons was obtained from the fitting parameter s_c using

$$\sigma_c = s_c \frac{k_B T}{L} \tag{3}$$

where k_B is the Boltzmann constant, T is the temperature, and L is the gas cell length. The cross section for electron loss from H^0 was obtained from σ_c and the fitting parameter R using

$$\sigma_l = \sigma_c R. \tag{4}$$

The uncertainties of the fitting parameters s_c and R provided the relative statistical uncertainties for the cross sections. For the relative cross sections, the major contributions to the uncertainty are the variation in the gas pressure during data taking and the statistical uncertainty in the counting statistics for the charge fractions. These uncertainties were used in weighting the data in the least-squares fits. In taking the pressure-dependence data, sufficient counts were accumulated in both the H^+ and H^0 channels to assure statistical uncertainties did not exceed 5%. Variation of the gas pressure during data accumulation was less than 5%.

Each data set was repeated at least once, and a weighted average of the cross sections from the separate measurements was used in all subsequent analysis.

Uncertainties in the absolute cross sections were obtained from the uncertainties in the fitting parameters, and also the normalization constants in equation (3). The major contribution to the uncertainty in the reported absolute cross sections is the uncertainty in the effective gas cell length. Although the physical length of the gas cell can be accurately measured, the effective length of the gas cell is different due to target gas streaming from the open entrance and exit apertures. The customary estimate of the effective target cell length is to add the diameters of the two apertures to the physical gas cell length [13, 14]. Such a correction for our gas cell yielded an effective length of 3.12 ± 0.36 cm. We have taken the uncertainty in the gas cell length to be equal to the length correction. The effective gas cell length only enters into the absolute normalization of the cross sections and does not affect the uncertainties for relative cross sections.

At high target pressures, the projectiles had multiple collisions with the target gas, and some projectiles may have scattered out of the acceptance angle of the detectors. However, a comparison of the total number of projectiles detected with no gas in the target cell to that with a high pressure (60 mTorr) in the cell showed no significant difference. In addition, electron capture cross sections obtained from a straight-line fit to the low-pressure portion of the data (single-collision conditions) agreed well with the capture cross sections obtained from the fit to the data over the whole pressure range. These two observations led to the conclusion that loss of projectiles through multiple scattering did not significantly affect the measured charge fractions.

3. Results

3.1. Molecular cross sections and test of additivity

In order to test the validity of the additivity rule and subsequently to obtain cross sections for atomic targets, it is advantageous to employ cross sections from hydrocarbon targets with a wide variety of numbers of constituent hydrogen and carbon atoms. Additionally, to minimize their relative uncertainties, the cross sections should be taken at identical energies with identical experimental apparatus and analysis. The present results provide such a set of cross sections. In table 1 are the cross sections for electron capture by 60–120 keV H^+ projectiles colliding with H_2, CH_4, C_2H_2, C_2H_4, C_2H_6, C_3H_6, and C_3H_8, and cross sections for electron loss from H^0 projectiles for the same targets are given in table 2. For C_2H_2 and C_3H_6 targets, no cross sections for electron capture or electron loss have been previously reported in this energy range; the present cross sections for these targets are displayed in figure 3. For the remaining target gases, previous workers have reported either electron capture or electron loss cross sections which at least partially overlap with the 60–120 keV energy range, namely: for H_2, capture [2, 10, 15–17] and loss [2, 10, 15, 18]; for CH_4, capture [2, 17, 19] and loss [2]; for C_2H_4, capture and loss [2]; for C_2H_6, capture [2, 19] and loss [2]; and for C_3H_8, capture [19]. In each case where earlier results were available for comparison, the present results are found to be in very good agreement with previous work. As a representative example of such a comparison, cross sections for the C_2H_6 target are shown in figure 4 along with the results of Toburen *et al* [2], Jones *et al* [19], and Eliot [20], and it can be seen that, for both capture and loss, the present results agree well with the previous measurements.

In our measurements of electron loss from H^0, it should be noted that the H^0 beam was formed within the target gas cell by a previous electron capture event by H^+. Some fraction of the H^0 projectiles formed in this manner will be in excited states when they undergo the second

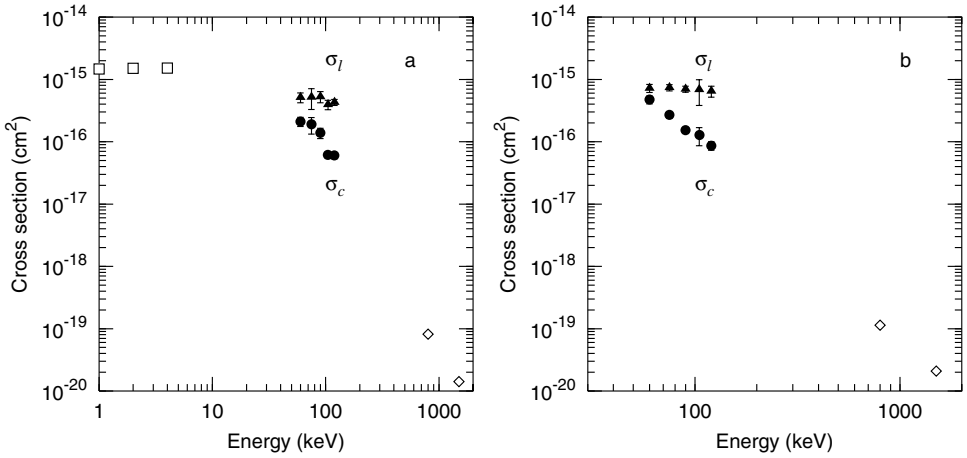

Figure 3. (a) Electron capture σ_c by H^+ and loss σ_l from H^0 in collisions with acetylene. Data shown: ● and ▲, present; □, Eliot [20] capture; ◇, Varghese *et al* [5] capture. (b) Electron capture σ_c by H^+ and loss σ_l from H^0 in collisions with propylene. Data shown: ● and ▲, present; ◇, Varghese *et al* [5] capture.

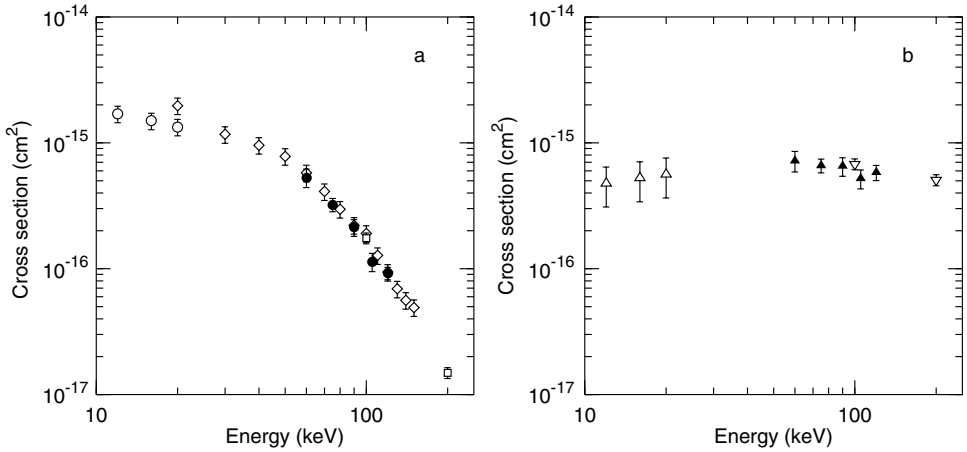

Figure 4. (a) Electron capture cross sections for H^+ colliding with ethane (C_2H_6). Data shown: ●, present; □, Toburen *et al* [2]; ◇, Jones *et al* [19]; ○, Eliot [20]. (b) Electron loss cross sections for H^0 colliding with ethane (C_2H_6). Data shown: ▲, present; ▽, Toburen *et al* [2]; △, Eliot [20].

collision in the gas cell and lose their electron. Thus, our electron loss cross sections should be understood to include contributions from both ground-state and excited H^0. Other groups who have measured electron loss from H^0 prepared the atomic hydrogen beam by neutralizing H^+ via electron capture in a separate neutralizing gas cell and then removing any remaining charged projectiles from the beam by electrostatic deflection [2, 18]. The electrostatic deflectors should have greatly reduced the number of excited atoms in the neutralized beams through Stark quenching; therefore, we would expect that the measurements of these groups were dominated by electron loss from the ground state of H^0. When we compared our loss cross sections with those of the other groups, we found no significant or systematic difference. We concluded, therefore, that excited states of H^0 must not contribute significantly to our loss cross sections.

To test the validity of the additivity rule in these collisions, a plane given by equation (1) was fitted to the measured cross sections for the seven target gases. The cross sections $\sigma_x^{C_nH_m}$

Table 1. Electron capture cross sections (in 10^{-16} cm^2) for H^+ colliding with hydrogen and hydrocarbon molecules.

	Energy (keV)				
Target	60	75	90	105	120
H_2	1.00 ± 0.11	0.392 ± 0.133	0.242 ± 0.027	0.142 ± 0.016	0.101 ± 0.012
CH_4	3.59 ± 0.76	1.68 ± 0.18	1.37 ± 0.32	0.819 ± 0.151	0.554 ± 0.065
C_2H_2	2.11 ± 0.36	1.88 ± 0.56	1.38 ± 0.26	0.615 ± 0.078	0.601 ± 0.066
C_2H_4	3.57 ± 0.66	2.32 ± 0.42	1.26 ± 0.13	0.953 ± 0.115	0.625 ± 0.085
C_2H_6	5.30 ± 0.88	3.22 ± 0.39	2.13 ± 0.32	1.14 ± 0.19	0.921 ± 0.105
C_3H_6	4.73 ± 0.69	2.69 ± 0.30	1.37 ± 0.17	1.27 ± 0.41	0.864 ± 0.134
C_3H_8	6.56 ± 0.70	3.88 ± 0.81	2.92 ± 0.31	1.28 ± 0.37	1.14 ± 0.14

Table 2. Electron loss cross sections (in 10^{-16} cm^2) for H^0 colliding with hydrogen and hydrocarbon molecules.

	Energy (keV)				
Target	60	75	90	105	120
H_2	1.54 ± 0.20	1.23 ± 0.51	1.09 ± 0.14	0.909 ± 0.102	0.992 ± 0.114
CH_4	4.78 ± 1.15	4.19 ± 0.44	4.68 ± 1.33	4.14 ± 0.89	3.74 ± 0.50
C_2H_2	5.14 ± 0.94	5.19 ± 1.90	5.29 ± 1.06	3.94 ± 0.67	4.29 ± 0.49
C_2H_4	6.67 ± 1.72	5.92 ± 1.25	5.20 ± 0.61	5.43 ± 0.72	4.62 ± 0.75
C_2H_6	7.19 ± 1.34	6.59 ± 0.83	6.52 ± 1.09	5.20 ± 0.89	5.82 ± 0.80
C_3H_6	7.23 ± 1.06	7.38 ± 0.83	6.97 ± 0.77	6.86 ± 3.06	6.48 ± 1.32
C_3H_8	9.40 ± 1.00	8.67 ± 2.22	8.62 ± 0.95	6.95 ± 2.09	7.12 ± 1.17

were fitted as functions of n and m, while the parameters adjusted in the fit were the two effective cross sections σ_x^{C} and σ_x^{H}, where the subscript x can be either c for capture or l for loss, and the superscripts C or H indicate an atomic carbon or atomic hydrogen target. If the cross sections are well described by the plane, we may conclude that the additivity rule holds. In order to display the three-dimensional dataset and fitted plane on a two-dimensional page, we rotate the fitted plane about the vertical axis until it is perpendicular to the plane of the paper. The data points are then projected onto the plane of the paper. The result of this projection is that a point $(n, m, \sigma_x^{\mathrm{C}_n\mathrm{H}_m})$ in three dimensions is mapped to a point $(D, \sigma_x^{\mathrm{C}_n\mathrm{H}_m})$ in two dimensions, where D is given by

$$D = n\cos\theta + m\sin\theta \tag{5}$$

and $\theta = \tan^{-1}(\sigma_x^{\mathrm{H}}/\sigma_x^{\mathrm{C}})$. By plotting the cross sections and fitting planes in this fashion, any deviations of the data from the fitted plane can be easily seen. The result of such a fit of the capture cross sections for 120 keV H^+ is shown in figure 5(a), and a fit for the 120 keV H^0 loss cross sections is shown in figure 5(b). As can be seen in the figures, the data are well described by the fitted planes, and similar fits were obtained for both capture and loss at the other energies as well. Since the cross sections fall closely to the planes, we conclude that the simple additivity rule holds reasonably well for these collisions.

As was mentioned in the introduction, additivity of cross sections is not the only way in which molecular cross sections may be scaled. Among the other scaling rules that have been proposed have been included the total number of atoms (making no distinction between atomic species), bond lengths, and the number of valence electrons. The cross sections reported in this paper scale with the number of valence electrons (taking one and four valence electrons

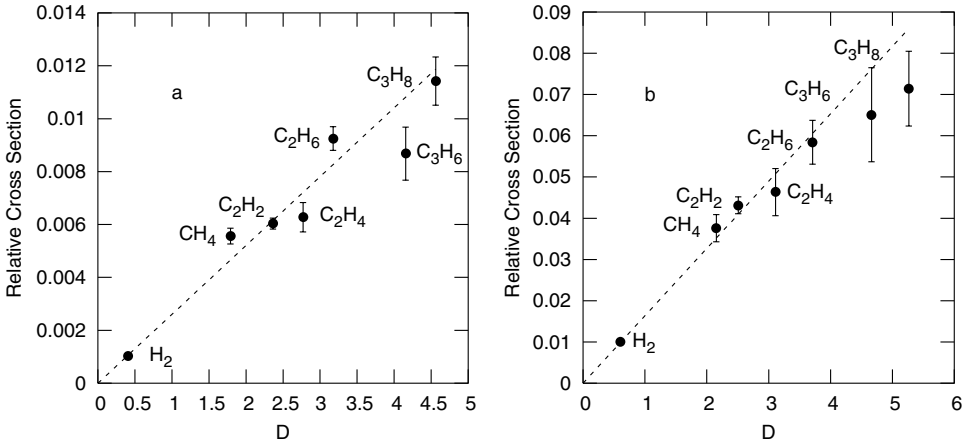

Figure 5. (a) Relative electron capture cross sections for 120 keV H^+ colliding with hydrogen and hydrocarbons. The line is the fitted plane of equation (1). The view has been rotated about the vertical axis, so the fitted plane is perpendicular to the plane of the paper. The quantity D is given by equation (5). (b) Relative electron loss cross sections for 120 keV H^0 colliding with hydrogen and hydrocarbons.

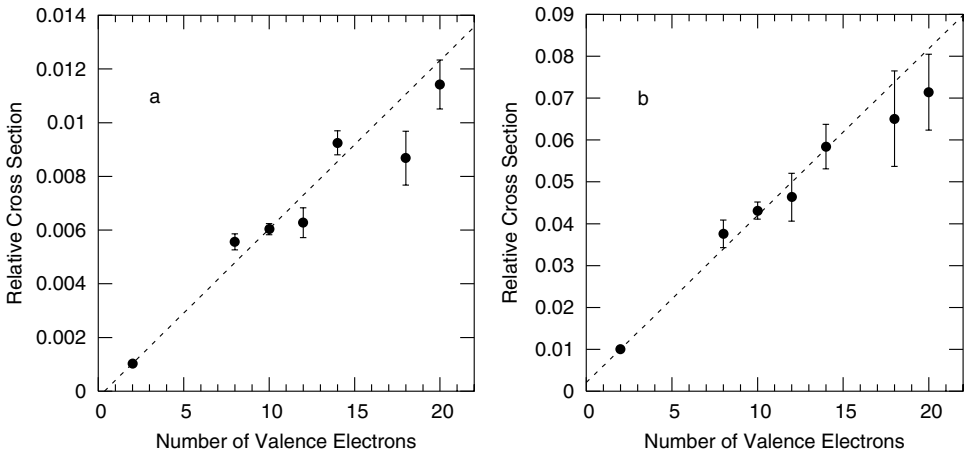

Figure 6. (a) Relative electron capture cross sections for 120 keV H^+ colliding with hydrogen and hydrocarbons as a function of the number of valence electrons. The dashed line is a linear fit to the data. (b) Relative electron loss cross sections for 120 keV H^0 colliding with hydrogen and hydrocarbons as a function of the number of valence electrons.

for hydrogen and carbon, respectively) about as well as they scale using the additivity rule, as may be seen in figure 6. The particular advantage of the additivity rule is that it allows atomic cross sections to be obtained from the molecular cross sections, as we discuss in the next section.

3.2. Effective atomic cross sections

Using the additivity rule, the fitting parameters for the planes described above can be interpreted to be the effective cross sections for capture or loss in collisions with free atomic carbon or

Table 3. Effective capture cross sections for H^+ colliding with H and C atoms.

Energy (keV)	σ_c^H (10^{-17} cm^2)	σ_c^C (10^{-17} cm^2)
60	5.16 ± 0.60	7.55 ± 1.21
75	3.61 ± 0.55	2.31 ± 1.41
90	1.27 ± 0.31	3.26 ± 0.90
105	0.72 ± 0.09	2.79 ± 0.40
120	0.53 ± 0.07	2.54 ± 0.32

Table 4. Effective loss cross sections for H^0 colliding with H and C atoms.

Energy (keV)	σ_l^H (10^{-17} cm^2)	σ_l^C (10^{-17} cm^2)
60	7.59 ± 0.96	11.5 ± 2.1
75	8.38 ± 0.97	8.30 ± 1.73
90	5.49 ± 0.75	13.6 ± 1.9
105	4.55 ± 0.50	15.9 ± 2.1
120	4.90 ± 0.57	15.5 ± 2.4

hydrogen targets. We will use the term 'effective' to emphasize that these cross sections rely upon the validity of the additivity rule. Effective cross sections for electron capture by protons colliding with atomic hydrogen and atomic carbon derived from the present experimental data are in table 3, and effective cross sections for electron loss from hydrogen atoms colliding with atomic hydrogen and atomic carbon are in table 4.

The effective capture and loss cross sections for atomic hydrogen targets are shown in figure 7 as the solid symbols. The open symbols in the figure are cross sections which have been obtained by other workers for actual atomic hydrogen targets for capture by H^+ [16, 21] and electron loss from H^0 [18]. Theoretical calculations for both processes are also shown. For electron capture we plot the first Born calculation of Belkić *et al* [22], and for electron loss the calculation of Bates and Griffing [23] is shown. It can be seen that the effective cross sections agree very well with both experiment and theory for atomic hydrogen targets.

The success of the additivity rule, in the 60–120 keV energy range, in yielding effective capture and loss cross sections for hydrogen that agree well with actual atomic hydrogen data and theory strongly suggests that the effective capture and loss cross sections for carbon will also accurately reflect actual atomic carbon cross sections. Figure 8 shows the effective capture and loss cross sections for atomic carbon targets as solid symbols. Also shown in the figure are the effective capture and loss cross sections of Toburen *et al* [2], which were also derived from molecular cross sections assuming the validity of the additivity rule.

Unlike the case with atomic hydrogen, no measurements have been made in this energy range for protons or hydrogen atoms colliding with atomic carbon targets, so direct comparisons between the effective cross sections and actual atomic carbon cross sections are not possible. However, following Stancil *et al* [24], we can estimate $H^+ + C$ electron capture cross sections as being equal to the electron capture cross section in the $C^+ + H$ collision at the same relative velocity. This is only an estimate, since the reversed $C^+ + H$ collision includes excited states of C that would not be present in the initial state of $H^+ + C$. In addition, the reversed collision excludes capture from inner shells of C and capture to excited states of H which would be included in an actual measurement of the electron capture cross section for $H^+ + C$ collisions. Despite these limitations, it can be seen from figure 8(a) that the present results agree well (with the exception of one out-lying point) with the kinematically reversed $C^+ + H$ cross sections [25, 26]. That there is such good agreement between these two quite different

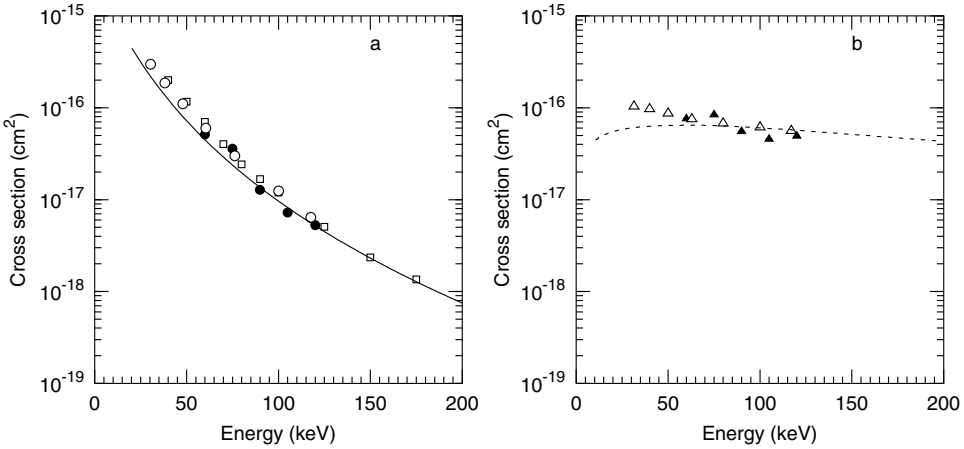

Figure 7. (a) Cross sections for electron capture by H^+ and (b) electron loss from H^0 colliding with atomic hydrogen, inferred using the additivity rule and compared with experimental cross sections measured on atomic hydrogen targets. For electron capture, the data shown are the following: ●, present; ○, McClure [16]; □, Wittkower *et al* [21]. The full curve is the first Born calculation for electron capture of Belkić *et al* [22]. For electron loss, the experimental data are the following: ▲, present; △, McClure [18]. The broken curve is the calculation of Bates and Griffing [23] for electron loss.

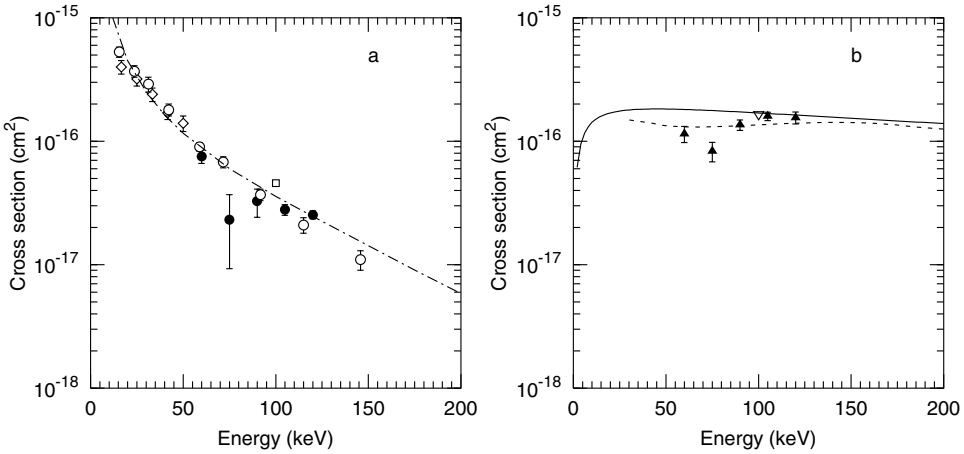

Figure 8. (a) Cross sections for electron capture by H^+ and (b) electron loss by H^0 colliding with atomic carbon targets inferred using the additivity rule. Experimental results shown for electron capture are the following: ●, present; □, Toburen *et al* [2]. Also shown are the kinematically reversed $C^+ + H$ capture cross sections: ◇, Phaneuf *et al* [25]; ○, Goffe *et al* [26]. The chain curve is the Bohr–Lindhard model of Knudsen *et al* [27] for electron capture in $H^+ + C$ collisions. For loss from H^0, experiment: ▲, present; ▽, Toburen *et al* [2]. The full curve is the Meron–Johnson model [28] for electron loss by H^0, and the broken curve is the estimate of electron loss of equation (6).

methods gives us confidence that the inferred atomic carbon cross sections of both methods are reliable. Also shown in figure 8(a) is the classical Bohr–Lindhard model of Knudsen *et al* [27], which has been successful in describing electron capture cross sections in this energy range, and it can be seen that the calculation agrees quite well with the effective capture cross sections, as well as with the kinematically reversed cross sections.

As was the case for the electron capture cross sections, there are no direct measurements of electron loss cross sections for H^0 colliding with atomic carbon to allow a comparison with the effective loss cross sections shown in figure 8(b). Toburen *et al* [2] also obtained effective loss cross sections from molecular targets using the additivity rule, and the present results agree well with theirs where the energy ranges overlap. Theoretical cross sections for electron loss from H^0 colliding with atomic carbon using the Born approximation have been reported by Levy [29] and Rule [30]. However, it is known that the Born approximation calculations tend to significantly overestimate loss cross sections for hydrogen atoms colliding with heavy targets at collision energies below about 1 MeV [29, 30]. Meron and Johnson [28] developed a semiempirical model for electron loss by H^0. Their model was based on parametrizing a free-collision approximation [31], and fitting the parameters to loss cross sections measured for He, Ne, Ar, and Xe targets. In figure 8(b), the solid curve shows a Meron and Johnson model calculation for an atomic carbon target, and it agrees with both the effective loss cross sections and those of Toburen *et al* [2] taken at 100 keV and above. At lower energies, the effective cross sections fall off rather earlier than the Meron and Johnson model.

Another, but cruder, estimate of the loss cross section is based on the observation that the Bohr–Lindhard model provides a good representation of the electron capture cross sections, and that the equilibrium neutral charge fraction in a carbon foil can be written (ignoring the small H^- contribution) as $f_\infty^0 = (1 + \sigma_l/\sigma_c)^{-1}$. Solving for σ_l yields

$$\sigma_l = \sigma_c\left(\frac{1}{f_\infty^0} - 1\right). \tag{6}$$

Thus, if f_∞^0 is known and σ_c can be calculated, the loss cross section σ_l can be obtained. The validity of this estimate is limited by the assumption that the equilibrium neutral charge fraction f_∞^0 in solid carbon is equal to the equilibrium fraction in a gas of free carbon atoms. In figure 8(b), the dashed curve is the result of such a calculation using the Bohr–Lindhard capture cross sections and the equilibrium H^0 charge fractions for carbon foils reported by Kreussler and Sizmann [32]. Despite the limitations mentioned above, this calculation agrees rather well with the effective loss cross sections and with the Meron–Johnson model.

4. Conclusion

We have reported measurements of electron capture by H^+ and electron loss from H^0 in collisions with molecular hydrogen and six hydrocarbon gases (CH_4, C_2H_2, C_2H_4, C_2H_6, C_3H_6, and C_3H_8) at energies ranging from 60 to 120 keV. Cross sections at only one energy (100 keV) had been previously reported in this energy range for C_2H_4 or for loss with a CH_4 target. No capture or loss cross sections for C_2H_2 or C_3H_6 and no loss cross sections for C_3H_8 had been previously reported in this intermediate energy range. It was found that both the capture and the loss cross sections reported here obey the simple additivity rule. The use of the additivity rule allowed the determination of effective cross sections for electron capture and electron loss in collisions with hydrogen and carbon atoms. The effective cross sections for atomic hydrogen were found to agree well with both experimental and theoretical cross sections for atomic hydrogen targets. Effective cross sections for atomic carbon were also obtained. Although no direct comparison of the effective cross sections with actual atomic carbon cross sections could be made, estimates from other, indirect, experiments and semi-empirical calculations indicate that the effective cross sections for atomic carbon are quite reasonable. In particular, there was agreement between cross sections estimated by kinematic reversal of $C^+ + H$ collisions and the effective cross sections derived from hydrocarbons using additivity. The agreement between these two quite independent, indirect techniques indicates

that both are capable of yielding atomic cross sections in situations where a direct measurement using an atomic target would be experimentally difficult.

The attraction of the additivity rule has always been its simplicity and its promise of allowing difficult atomic cross sections to be extracted from less troublesome molecular targets. The success of the additivity rule in this experiment suggests that it is a worthwhile tool for obtaining atomic cross sections, provided that its validity has first been established for the collisions and processes being studied.

Acknowledgments

This work was supported in part by the University of South Alabama Research Council and the University of South Alabama University Committee on Undergraduate Research. We thank A J K Pearce, S E Gardner, and C D Gunn for assistance with some of the data taking. We also wish to thank the anonymous referees for helpful suggestions regarding some experimental aspects.

References

[1] Kusakabe T, Asahina K, Iida A, Tanaka Y, Li Y, Hirsch G, Buenker R J, Kimura M, Tawara H and Nakai Y 2000 *Phys. Rev.* A **62** 062715
[2] Toburen L H, Nakai M Y and Langley R A 1968 *Phys. Rev.* **171** 114–22
[3] Varghese S L, Bissinger G, Joyce J M and Laubert R 1980 *Nucl. Instrum. Methods* **170** 269–73
[4] Bissinger G, Joyce J M, Lapicki G, Laubert R and Varghese S L 1982 *Phys. Rev. Lett.* **49** 318–22
[5] Varghese S L, Bissinger G, Joyce J M and Laubert R 1985 *Phys. Rev.* A **31** 2202–9
[6] Varghese S L 1987 *Nucl. Instrum. Methods Phys. Res.* B **24/25** 40–3
[7] Dillingham T R, Doughty B M, Hall J M, Tipping T N, Sanders J M and Shinpaugh J L 1989 *Nucl. Instrum. Methods Phys. Res.* B **40/41** 40–3
[8] Rottmann L M, Bruch R, Neill P, Drexler C, DuBois R D and Toburen L H 1992 *Phys. Rev.* A **46** 3883–8
[9] Watson R L, Peng Y, Horvat V and Kim G J 2003 *Phys. Rev.* A **67** 022706
[10] Stier P M and Barnett C F 1956 *Phys. Rev.* **103** 896–907
[11] Allison S K 1958 *Rev. Mod. Phys.* **30** 1137–68
[12] McDaniel E W, Mitchell J B A and Rudd M E 1993 *Atomic Collisions: Heavy Particle Projectiles* (New York: Wiley)
[13] Toburen L H, Nakai M Y and Langley R A 1968 *Oak Ridge National Laboratory Technical Report* ORNL-TM-1988 appendix II
[14] Tawara H and Russek A 1973 *Rev. Mod. Phys.* **45** 178–229
[15] Barnett C F and Reynolds H K 1958 *Phys. Rev.* **109** 355–9
[16] McClure G W 1966 *Phys. Rev.* **148** 47–54
[17] Rudd M E, DuBois R D, Toburen L H, Ratcliffe C A and Goffe T V 1983 *Phys. Rev.* A **28** 3244–57
[18] McClure G W 1968 *Phys. Rev.* **166** 22–9
[19] Jones M L, Doughty B M, Dillingham T R and Jones T A 1985 *Nucl. Instrum. Methods Phys. Res.* B **10/11** 142–5
[20] Eliot M 1977 *J. Physique* **38** 21–7
[21] Wittkower A B, Ryding G and Gilbody H B 1966 *Proc. Phys. Soc.* **89** 541–6
[22] Belkić D, Saini S and Taylor H S 1987 *Phys. Rev.* A **36** 1601–17
[23] Bates D R and Griffing G W 1955 *Proc. Phys. Soc.* **68** 90–6
[24] Stancil P C, Gu J P, Havener C C, Krstić P S, Schultz D R, Kimura M, Zygelman B, Hirsch G, Buenker R J and Bannister M E 1998 *J. Phys. B: At. Mol. Opt. Phys.* **31** 3647–63
[25] Phaneuf R A, Meyer F W and McKnight R H 1978 *Phys. Rev.* A **17** 534–45
[26] Goffe T V, Shah M B and Gilbody H B 1979 *J. Phys. B: At. Mol. Phys.* **12** 3763–73
[27] Knudsen H, Haugen H K and Hvelplund P 1981 *Phys. Rev.* A **23** 597–610
[28] Meron M and Johnson B M 1990 *Phys. Rev.* A **41** 1365–74
[29] Levy H 1969 *Phys. Rev.* **185** 7–15
[30] Rule D W 1977 *Phys. Rev.* A **16** 19–25
[31] Dewangan D P and Walters H R J 1978 *J. Phys. B: At. Mol. Phys.* **11** 3983–4017
[32] Kreussler S and Sizmann R 1982 *Phys. Rev.* B **26** 520–9